

Roles of Hund's Rule and Hybridization in the Two-orbital Model for High- T_c Superconductivity in the Bilayer Nickelate

Xing-Zhou Qu,^{1,2,*} Dai-Wei Qu,^{1,2,*} Wei Li,^{2,3,4,†} and Gang Su^{1,4,‡}

¹Kavli Institute for Theoretical Sciences, University of Chinese Academy of Sciences, Beijing 100190, China

²CAS Key Laboratory of Theoretical Physics, Institute of Theoretical Physics, Chinese Academy of Sciences, Beijing 100190, China

³Hefei National Laboratory, Hefei 230088, China

⁴CAS Center for Excellence in Topological Quantum Computation, University of Chinese Academy of Sciences, Beijing 100190, China

The intriguing interplay between the two e_g orbitals in the high- T_c nickelate superconductor $\text{La}_3\text{Ni}_2\text{O}_7$ is studied via the density matrix renormalization group (DMRG) and finite- T thermal tensor-network calculations. We consider a bilayer t - J model that incorporates both $d_{x^2-y^2}$ and d_{z^2} orbitals, as well as inter-orbital hybridization and ferromagnetic Hund's rule coupling. Our DMRG calculations reveal that both orbitals exhibit algebraic superconductive (SC) pairing correlations in the ground state, with the former being stronger than the latter. To confirm the dominant $d_{x^2-y^2}$ -orbital SC order, we compute the pairing susceptibility χ_{SC} , and find a power-law divergence of χ_{SC} below $T_c^* \simeq 0.03t_c$, with t_c being the intralayer hopping of the $d_{x^2-y^2}$ orbital. Regarding the d_{z^2} orbitals, their finite- T χ_{SC} results show weaker divergence and suggest lower T_c^* . We delve deeper into the intricate interplay between Hund's rule coupling and inter-orbital hybridization by tuning the two parameters, and reveal two distinct SC phases dominated by Hund's rule and hybridization, respectively, separated by a non-SC regime. Our results treat the two e_g orbitals in a bilayer model on an equal footing, and clarify the essential roles of Hund's rule and hybridization in the formation of SC order in the pressurized nickelate $\text{La}_3\text{Ni}_2\text{O}_7$.

Introduction.— The discovery of nearly 80 K superconductivity (SC) in the pressurized Ruddlesden-Popper bilayer perovskite $\text{La}_3\text{Ni}_2\text{O}_7$ [1] has received considerable research interests in both experiment [2–8] and theory [9–54]. Currently, a consensus has more or less reached that the bilayer structure and orbital selectivity are two key factors in the formation of superconductivity (SC) in the strongly correlated compound $\text{La}_3\text{Ni}_2\text{O}_7$. From a strong coupling point of view, the interlayer antiferromagnetic (AF) coupling between d_{z^2} orbitals can provide the driven force of SC pairing [22–27, 31], and both $d_{x^2-y^2}$ and d_{z^2} orbitals can benefit from such interlayer coupling for forming SC order.

To be specific, the d_{z^2} orbitals can pair up through interlayer AF interactions but lacks coherence due to the low hole density and small hopping. Although it has been proposed that the d_{z^2} pairs can move coherently through hybridization with the itinerant $d_{x^2-y^2}$ orbital [15, 27, 31, 47], it is unclear whether the d_{z^2} orbitals could gain sufficiently high T_c . The recent DMRG and infinite projected-entangled pair state (iPEPS) studies [26] point out the large t_\perp inherent in d_{z^2} orbitals can also lead to strong Pauli blocking [55] that diminishes the SC order in d_{z^2} orbital.

In a different, $d_{x^2-y^2}$ scenario, these itinerant orbitals within each layer are regarded to play a dominant role in forming the SC order [22, 24, 26, 33, 37, 38, 40, 44, 48]. Distinct to the d_{z^2} orbitals, the $d_{x^2-y^2}$ ones have sufficient hole density (near quarter filling) and strong intralayer hopping with relatively wide bands. However, $d_{x^2-y^2}$ orbitals do not have significant interlayer hopping and thus the magnetic mediation for SC pairing is lacking. Nevertheless, the significant ferromagnetic (FM) Hund's rule coupling $J_H \sim 1$ eV come to rescue [16, 19, 32, 46], which can transfer the interlayer AF couplings from d_{z^2} interlayer dimer to the $d_{x^2-y^2}$ orbitals

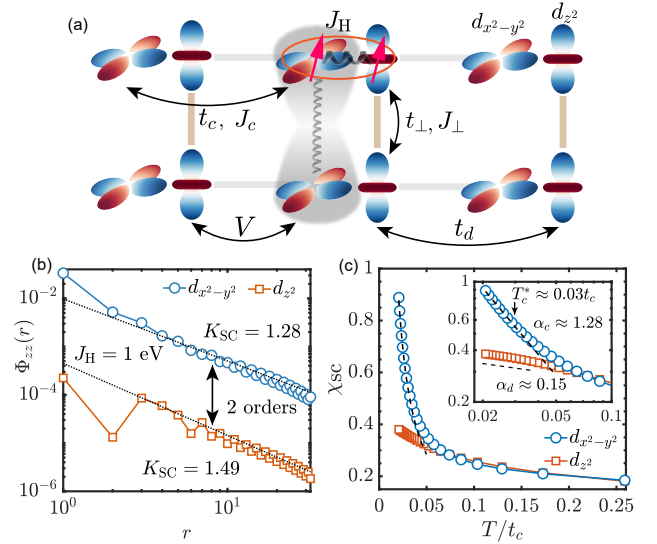


FIG. 1. (a) The two-orbital bilayer t - J model consists of several hopping and couplings, including two intralayer t - J model of the $d_{x^2-y^2}$ orbital (t_c, J_c), d_{z^2} orbital with interlayer interactions (t_\perp, J_\perp) and intralayer hopping t_d . Additionally, there are intralayer hybridization between the nearest-neighbor $d_{x^2-y^2}$ and d_{z^2} orbitals (V), on-site Hund's rule coupling (J_H). (b) The SC pairing correlations $\Phi_{zz}(r)$ between two $d_{x^2-y^2}$ and d_{z^2} orbitals, with r denoting the distance between two rung singlets. We find $\Phi_{zz}(r)$ is mainly contributed by the $d_{x^2-y^2}$ orbitals. (c) The pairing susceptibility $\chi_{\text{SC}}(T)$ computed for each orbital, which divergence algebraically as $\chi_{\text{SC}} \sim 1/T^{\alpha_c}$ (with $\alpha_c \simeq 1.25$) for $d_{x^2-y^2}$ below $T_c^* \approx 0.03t_c$. The χ_{SC} for d_{z^2} orbital exhibits very weak divergence. Throughout the work, we use the blue-green color scheme to label the $d_{x^2-y^2}$ orbital, and the orange-red color scheme to label the d_{z^2} orbital.

and render the latter strong pairing force. Under the large

J_H assumption, the d_{z^2} orbital can be safely integrated out, giving rise to a single t - J - J_\perp model with robust and high- T_c SC [22, 26].

Currently, there is intensive ongoing research aimed at determining which of the two e_g orbitals, $d_{x^2-y^2}$ or d_{z^2} , is primarily responsible for the SC order. In this study, we take both orbitals into account and consider the inter-orbital hybridization and Hund's rule couplings simultaneously, to conduct a comparative study between the two scenarios. We employ state-of-the-art tensor network simulations, including the $T = 0$ DMRG and $T > 0$ tensor renormalization group [56–58] to investigate the two-orbital bilayer t - J model with realistic model parameters [9], aiming to address the intriguing interplay between two e_g orbitals unbiasedly.

Our results reveal that, both Hund's rule coupling J_H and hybridization V can stabilize robust SC order, as characterized by the algebraic pairing correlations and divergent SC

susceptibilities. In either case, we find the $d_{x^2-y^2}$ orbital is responsible for the robust SC with algebraic pairing correlation and higher T_c^* estimated from pairing susceptibility. Moreover, we find Hund's rule coupling J_H and hybridization V can each stabilize SC order in the the hybridization dominant and Hund dominant SC phases, respectively. They are separated by an intermediate regime with absence of SC order. In both hybridization and Hund dominant regimes, the inter-layer magnetic correlations between $d_{x^2-y^2}$ orbitals are more pronounced. We ascribe this to the magnetically mediated interlayer pairing mechanism via the single-band t - J - J_\perp model on a mixed-dimensional (mixD) bilayer lattice [22, 26].

Two-orbital bilayer t - J model for $\text{La}_3\text{Ni}_2\text{O}_7$.— To comprehensively understand the pairing mechanism in the bilayer nickelate $\text{La}_3\text{Ni}_2\text{O}_7$, we study the following two-orbital t - J model whose Hamiltonian reads

$$\begin{aligned}
 H = & - t_c \sum_{\langle i,j \rangle, \mu, \sigma} \left(c_{i,\mu,\sigma}^\dagger c_{j,\mu,\sigma} + H.c. \right) + J_c \sum_{\langle i,j \rangle, \mu} \left(\mathbf{S}_{i,\mu}^c \cdot \mathbf{S}_{j,\mu}^c - \frac{1}{4} n_{i,\mu}^c n_{j,\mu}^c \right) \\
 & - t_\perp \sum_{i,\sigma} \left(d_{i,\mu=1,\sigma}^\dagger d_{j,\mu=-1,\sigma} + H.c. \right) + J_\perp \sum_i \left(\mathbf{S}_{i,\mu=1}^d \cdot \mathbf{S}_{i,\mu=-1}^d - \frac{1}{4} n_{i,\mu=1}^d n_{i,\mu=-1}^d \right) \\
 & - t_d \sum_{\langle i,j \rangle, \mu, \sigma} \left(d_{i,\mu,\sigma}^\dagger d_{j,\mu,\sigma} + H.c. \right) - V \sum_{\langle i,j \rangle, \mu, \sigma} \left(c_{i,\mu,\sigma}^\dagger d_{j,\mu,\sigma} + H.c. \right) - J_H \sum_{i,\mu} \mathbf{S}_{i,\mu}^c \cdot \mathbf{S}_{i,\mu}^d + \varepsilon_c \sum_{i,\mu} n_{i,\mu}^c + \varepsilon_d \sum_{i,\mu} n_{i,\mu}^d
 \end{aligned}$$

where the annihilation operator for the $d_{x^2-y^2}$ (d_{z^2}) electron at site i , layer $\mu = \pm 1$, and spin $\sigma = \{\uparrow, \downarrow\}$ is denoted by $c_{i,\mu,\sigma}$ ($d_{i,\mu,\sigma}$). The spin of the $d_{x^2-y^2}$ (d_{z^2}) electron at site i and layer μ is represented by $\mathbf{S}_{i,\mu}^c$ ($\mathbf{S}_{i,\mu}^d$), and the density operator is denoted by $n_{i,\mu}^c$ ($n_{i,\mu}^d$). The parameter t_c (t_d) labels the intralayer hopping of the $d_{x^2-y^2}$ (d_{z^2}) orbital, and the intralayer spin coupling between the $d_{x^2-y^2}$ orbital is denoted as J_c , while that of d_{z^2} is negligibly small as $J_d \sim t_d^2/t_c^2 \ll 1$. The interlayer hopping and coupling of the d_{z^2} orbital are labeled as t_\perp and J_\perp , respectively. The inter-site hybridization V and the onsite Hund's rule coupling J_H between the two e_g orbitals, where we suppose a rotational invariant form [59]. ε_c and ε_d label the site energies of the $d_{x^2-y^2}$ and the d_{z^2} orbitals, respectively.

To select realistic model parameters, we set $t_c = 0.483$ eV, $t_\perp = 0.635$ eV, $t_d = 0.110$ eV, $V = 0.239$ eV, $\varepsilon_c = 0.776$ eV, and $\varepsilon_d = 0.409$ eV, according to the tight-binding model from the density functional theory calculations [9]. With an appropriately chosen Hubbard $U = 4$ eV [16, 32], we estimate the spin couplings as $J_c \simeq 4t_c^2/U = 0.233$ eV and $J_\perp \simeq 4t_\perp^2/U = 0.403$ eV. The Hund's rule coupling J_H is increased in the calculations, with strength up to about 1 eV ($\sim 2.5J_\perp$) relevant for the compound. The electron filling is fixed as $3/8$, i.e., $n_e = 1.5$, per site, and the orbital energy ε_c and ε_d control its distribution within the two e_g orbitals.

Zero- and finite-temperature tensor network methods.—

We exploit the density matrix renormalization group (DMRG) [60, 61] method at zero temperature and tangent-space tensor renormalization group (tanTRG) [58] method at finite temperature. Non-abelian and abelian symmetries are implemented with the tensor library QSpace [62, 63] and ITensor [64, 65] libraries. In both calculations, we consider the $2 \times L_x$ (with L_x up to 64) two-orbital ladder that is mapped into a quasi-1D chain with long-range interactions. We retain up to $D^* = 4,500$ $U(1)_{\text{charge}} \times SU(2)_{\text{spin}}$ multiplets or $D = 9,000$ $U(1)_{\text{charge}} \times U(1)_{\text{spin}}$ states in DMRG simulations. The results are well converged with typical truncation error $\epsilon \sim 10^{-6}$.

In finite- T tanTRG calculations, we consider system size $L_x = 24$. To compute the pairing susceptibility, a small pairing field is applied that breaks the electron number conservation. Therefore, we use $\mathbb{Z}_{2,\text{charge}} \times SU(2)_{\text{spin}}$ symmetry and retain up to $D^* = 2000$ multiplets (equivalent to ~ 5200 states), with typical truncation error $\epsilon \sim 10^{-4}$. To control the electron density, a chemical potential term $-\mu N_{\text{tot}}$ is added to the Hamiltonian, with N_{tot} the total electron number. We fine tune the parameter μ so that the two-orbital system is approximately at $3/8$ filling at low temperature.

Orbital selective SC order.— We first investigate the orbital selective behaviors of the two, namely, $d_{x^2-y^2}$ and d_{z^2} orbitals with realistic parameters indicated above. We compute the pairing correlation $\Phi_{zz}(r)$ at $T = 0$ and SC suscepti-

bility χ_{SC} at $T > 0$. In Fig. 1(b), we show the interlayer pair correlation $\Phi_{zz}(r) = \langle \Delta_i^\dagger \Delta_j \rangle$, where interlayer pairing $\Delta_i^\dagger = \frac{1}{\sqrt{2}} \sum_{\mu=\pm 1} c_{i,\mu,\uparrow}^\dagger c_{i,\mu,\downarrow}^\dagger$ (for $d_{x^2-y^2}$ orbital) and distance $r \equiv |j - i|$. When switched from $d_{x^2-y^2}$ to the d_{z^2} orbital, we replace $c_{i,\mu,\sigma}$ with $d_{i,\mu,\sigma}$. The pairing susceptibility $\chi_{SC}(T)$ is defined as $\chi_{SC} = \frac{1}{L_x} \partial \langle \Delta_{tot} \rangle / \partial h_p$, computed at finite temperature and by applying a small pairing field $-h_p \Delta_{tot}$ to the system, with $\Delta_{tot} = \frac{1}{2} \sum_{i=\frac{1}{4}L_x}^{\frac{3}{4}L_x} [\Delta_i + (\Delta_i)^\dagger]$ and small $h_p = 0.002$ in practice.

In Fig. 1(b) and (c), we present results of the pair correlations $\Phi_{zz}(r)$ and the superconducting susceptibility $\chi_{SC}(T)$ for both e_g orbitals. From Fig. 1(b), we find that the $d_{x^2-y^2}$ orbitals exhibit much stronger pairing correlations, with two orders of magnitude larger than that of the d_{z^2} orbital. From the power-law fitting, we find the $K_{SC} \simeq 1.28$ for the $d_{x^2-y^2}$ orbital, suggesting a divergent pairing susceptibility. We also notice that although the magnitude is rather weak, the pairing correlation of d_{z^2} orbital also follow a algebraic scaling, but with a slightly larger $K_{SC} \simeq 1.49$. Despite the significant difference in the magnitude, the proximity effect renders similar Luttinger parameter K_{SC} for the two orbitals.

Therefore, we turn to finite-temperature simulations to determine which orbital is primarily responsible for the high superconducting transition temperature T_c . We compute the pairing susceptibilities $\chi_{SC}(T)$, which characterize the SC instabilities in the two e_g orbitals. In Fig. 1(c), we find that for either $d_{x^2-y^2}$ or d_{z^2} orbital, a power-law divergence of $\chi_{SC} \sim 1/T^\alpha$ appears at low temperature, which is consistent with the DMRG results of Luttinger parameters $K_{SC} < 2$. Similar to the ground-state results, here we also find much stronger SC pairing response in the $d_{x^2-y^2}$ orbital, reflected in its more significant magnitude and clearly greater exponent $\alpha_c \gg \alpha_d$ of the d_{z^2} orbital. From the behaviors of $\chi_{SC}(T)$ we estimate $T_c^* \simeq 0.03t_c$, which represents a high SC transition temperature in the order of 10^2 K.

Magnetically mediated SC pairing promoted by Hund's rule coupling.— To further reveal the role of Hund's rule coupling J_H , we tune J_H from small to realistic values of about 1 eV. In Fig. 2(a), we find a large $K_{SC} > 2$ for small J_H , suggesting the absence of SC order. Only for $J_H \gtrsim 1$ eV, the (quasi long-range) SC order with $K_{SC} < 2$ can be realized, from which we draw a conclusion that a sufficient J_H is essential for stabilizing the SC order.

In Fig. 2(b), we present various spin-spin correlations, including the on-site inter-orbital correlation $F_{c,d} = \frac{1}{2L_x} \sum_{i,\mu} \langle \mathbf{S}_{i,\mu}^c \cdot \mathbf{S}_{i,\mu}^d \rangle$, as well as interlayer $F_\perp^c \equiv \frac{1}{L_x} \sum_i \langle \mathbf{S}_{i,\mu=1}^c \cdot \mathbf{S}_{i,\mu=-1}^c \rangle$ and intralayer spin correlations $F_\parallel^c \equiv \frac{1}{2(L_x-1)} \sum_{i,\mu} \langle \mathbf{S}_{i,\mu}^c \cdot \mathbf{S}_{i+1,\mu}^c \rangle$ in the $d_{x^2-y^2}$ orbital. Our analysis of these spin correlations has led us to the conclusion that the on-site $F_{c,d}$ indicates FM correlation in the large J_H regime, which is crucial for transferring the interlayer AF correlations F_\perp^c from the d_{z^2} orbitals to the $d_{x^2-y^2}$ orbitals. As J_H increases, F_\perp^c also increases continuously, and in the superconducting state, the magnitude of the transferred inter-

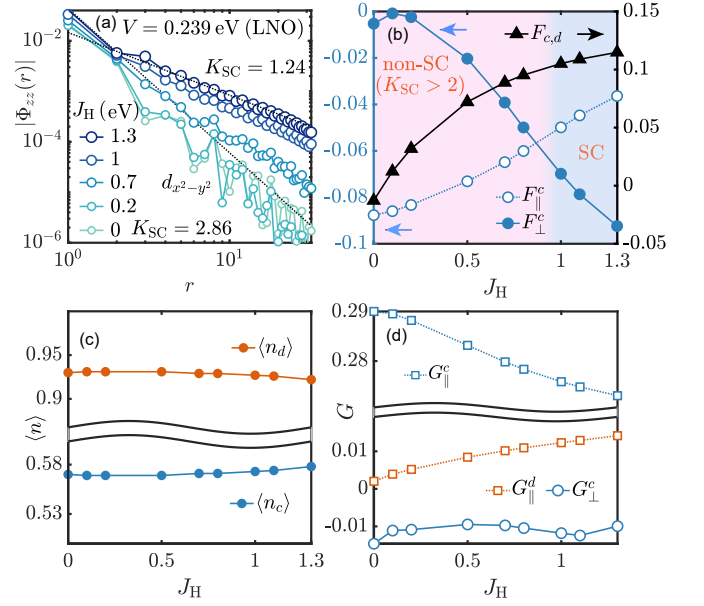


FIG. 2. (a) Interlayer pair correlation for $d_{x^2-y^2}$ orbital with various Hund's rule coupling J_H . (b) Inter-orbital on-site spin correlation $F_{c,d}$, interlayer spin correlation F_\perp^c , and intralayer spin correlation F_\parallel^c . The SC and non-SC regimes are marked with different background colors. (c) shows the electron densities in the two e_g orbitals and (d) plots the Green's function of each orbital (see definition in the main text).

layer correlation F_\perp^c becomes even greater than the intralayer spin correlations mediated by super exchange. A realistic J_H slightly above 1 eV has already made the interlayer AF correlation about twice as large as the intralayer spin correlations of the $d_{x^2-y^2}$ orbitals.

In Fig. 2(c), we further show the electron densities $n_{c,d}$ and the single-particle Green's function $G_{\parallel,\perp}$ for the $d_{x^2-y^2}$ and d_{z^2} orbitals. The intralayer Green's function is defined as $G_\parallel^\alpha \equiv \frac{1}{2(L_x-1)} \sum_{i,\mu,\sigma} \langle \alpha_{i,\mu,\sigma}^\dagger \alpha_{i+1,\mu,\sigma} \rangle$ between nearest-neighbor sites within each layer, with $\alpha = \{c, d\}$ denoting the two e_g orbital. The interlayer Green's function can be similarly defined, $G_\perp^c \equiv \frac{1}{L_x} \sum_{i,\sigma} \langle c_{i,\mu=1,\sigma}^\dagger c_{i,\mu=-1,\sigma} \rangle$, which reflects the kinetic energy of electron hopping between two layers. The results in Fig. 2(c) indicate that the d_{z^2} is nearly half-filled with only few holes, in distinction with the quarter-filled $d_{x^2-y^2}$ orbitals with $n_c \approx 0.58$. The Green's function results in Fig. 2(d) further indicate that the d_{z^2} electrons are rather localized with very small intralayer kinetic energy as $G_\parallel^d \ll G_\parallel^c$, while the $d_{x^2-y^2}$ orbitals are itinerant and in principle moving coherently within each layer (large G_\parallel^c), but not across two layers (negligible G_\perp^c).

Overall, the results presented in Fig. 2 provide clear evidence that the d_{z^2} orbital is localized and can be regarded as a local moment. In contrast, the $d_{x^2-y^2}$ electrons are itinerant, strongly correlated, and is mainly responsible for the robust SC order. The Hund's rule coupling J_H plays an essential role in forming the robust SC order by transferring AF interlayer

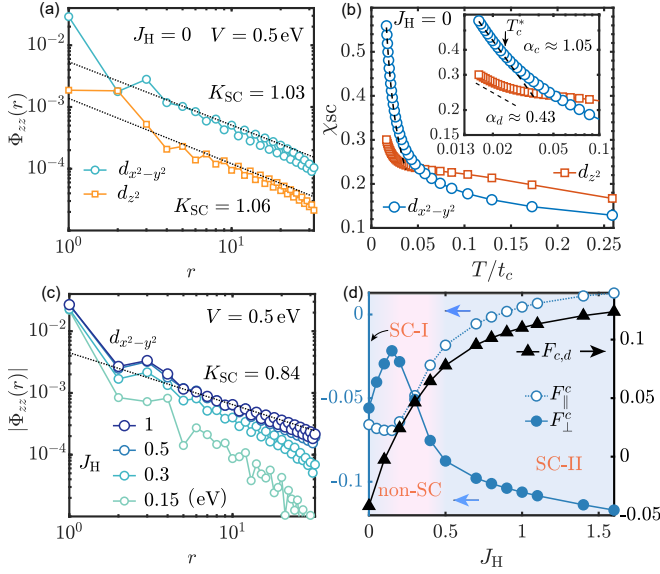


FIG. 3. (a) Interlayer pair correlation of $d_{x^2-y^2}$ and d_{z^2} orbitals with hybridization $V = 0.5$ eV and $J_H = 0$. Quasi-long range SC order is revealed by the computed algebraic pairing correlation with $K_{SC} \simeq 1.03$. (b) Pairing susceptibilities of the two orbitals at finite temperature. (c) Interlayer pair correlation of $d_{x^2-y^2}$ orbital at $V = 0.5$ eV and various Hund's rule couplings $J_H > 0.15$ eV, where SC order is firstly suppressed and then appear again by J_H . (d) Spin correlation $F_{c,d}$ between two e_g orbitals on the same site, interlayer spin correlation F_{\perp}^c and intralayer spin correlation F_{\parallel}^c . The SC-I originates from pure hybridization while SC-II is dominant by the Hund's rule, with an intermediate non-SC regime between the two SC phases also highlighted.

spin exchanges from the d_{z^2} to the $d_{x^2-y^2}$ orbitals.

Interplay between inter-orbital hybridization and Hund's rule coupling.— In Fig. 2(a,b), we find the absence of the SC order (with $K_{SC} > 2$) when J_H is switched off, which may be ascribed to the relatively small inter-orbital hybridization V . In Fig. 3 we artificially introduce an enhanced $V = 0.5$ eV, twice as large as the realistic hybridization in the $\text{La}_3\text{Ni}_2\text{O}_7$ compound, and conducted tensor-network calculations of pairing correlations and susceptibilities.

In Fig. 3(a) we observe that $\Phi_{zz}(r)$ falls into the algebraic scaling, with a $K_{SC} \simeq 1.03$ ($d_{x^2-y^2}$ orbital) that corresponds to SC order. The correlations of the Δ orbital are significantly smaller, yet with a similar Luttinger parameter of $K_{SC} \sim 1$, which can be attributed to the proximity effect. To determine which orbital is responsible for the high transition temperature T_c , we show the pairing susceptibility χ_{SC} in Fig. 3(b), from which we find that χ_{SC} of the $d_{x^2-y^2}$ orbital scales as $1/T^{\alpha_c}$ with $\alpha_c \approx 2 - K_{SC}$ below the estimated transition temperature $T_c^* \simeq 0.02t_c$. On the other hand, the χ_{SC} of the d_{z^2} orbital is much smaller, and shows only weak divergence with α_d much smaller than α_c . We expect χ_{SC} of the d_{z^2} orbital to also diverge as $1/T^{2-K_{SC}}$, possibly at a lower transition temperature T_c^* . Based on the finite- T results, we thus attribute the high- T_c SC in the two-orbital system primarily to the $d_{x^2-y^2}$ band.

The results in Fig. 3(a,b) show that the SC order can

indeed be stabilized by sufficiently strong inter-orbital hybridization. Nevertheless, the Hund's rule coupling arising from the atomic scale is inevitable and should be considered. In Fig. 3(c) we switch on the Hund's rule coupling J_H and find the SC order is quickly suppressed by relatively small $J_H \simeq 0.15$ eV. After that, the Hund's rule coupling J_H gradually establishes a robust SC order for $J_H \geq 0.5$ eV. This can be understood by checking the spin correlation data in Fig. 3(d), where onsite inter-orbital spin correlation $F_{c,d}$ changes its sign from AF (driven by hybridization) to FM (Hund's rule dominant). In the intermediate regime, Hund's rule competes with the hybridization and a non-SC regime appears, where $F_{c,d}$ is very small and $d_{x^2-y^2}$ orbital has also weak interlayer AF correlations. Once the Hund's rule coupling J_H is sufficiently strong, the interlayer AF spin correlations F_{\perp}^c can be effectively passed from the d_{z^2} to $d_{x^2-y^2}$ orbital, which surpasses the intralayer correlation F_{\parallel}^c and mediate a robust SC pairing.

Discussion and outlook.— In this work, we consider a two-orbital bilayer model with both inter-orbital hybridization and Hund's rule coupling, and their intriguing interplay. Our zero- and finite-temperature results show that the $d_{x^2-y^2}$ orbital exhibits strong SC pairing and is mainly responsible for the high- T_c SC in the two-orbital system. With realistic model parameters, we find that the $d_{x^2-y^2}$ orbitals are itinerant within each layer, and d_{z^2} orbitals is nearly half-filled and localized. The Hund's rule plays an essential role in form the SC order, which effectively transfers the AF correlations from the d_{z^2} to $d_{x^2-y^2}$ orbitals. Our results fully support the single-band t - J - J_{\perp} model [22, 26, 51] consists of $d_{x^2-y^2}$ orbitals is a minimal pathway for understanding the interlayer-pairing SC order in the pressurized $\text{La}_3\text{Ni}_2\text{O}_7$.

With this understanding, we are well-positioned to address the relevance of the σ -bond metallization mechanism in the context of SC order in bilayer nickelates. We fine-tune the site energies of the two e_g orbitals, ε_c and ε_d , and find that reducing the holes in the d_{z^2} orbital (which are transferred to the $d_{x^2-y^2}$ orbital) is beneficial, rather than detrimental, to the formation of a robust SC order. Our findings are supported by detailed computational results presented in the Supplementary Materials [66], which demonstrate that the SC order can be enhanced by tuning d_{z^2} orbital to approach half-filled, namely, towards insularization instead of metallization of the d_{z^2} band.

To extend the present study, it is essential to investigate the impact of hybridization in the Hund's rule dominant SC regime. In Fig. 2(b), we notice that the non-SC regime is extensive and spans up to $J_H \approx 0.9$ eV for a relatively modest (and realistic) $V = 0.239$ eV. However, the non-SC regime becomes significantly reduced for larger $V = 0.5$ eV. This raises an intriguing question about the interplay between hybridization and Hund's rule, which may be more intricate than simply competing. A possibility is that in the strong Hund's rule coupling regime, the virtual hopping with V can provide additional spin correlations between the $d_{x^2-y^2}$ and nearest-neighbor d_{z^2} orbitals, thereby enhancing the magnetic me-

diated pairing. We leave this topic in future studies, potentially using a Hubbard model that better accounts for the effects of inter-orbital hybridization.

Acknowledgments.— The authors are indebted to Jialin Chen, Xin-Wei Yi, Congjun Wu, and Fan Yang for stimulating discussions. This work was supported by the National Natural Science Foundation of China (Grant Nos. 12222412, 11834014, 11974036, 12047503, 12074031, 12174317, and 12234016), Strategic Priority Research Program of CAS (Grant No. XDB28000000), Innovation Program for Quantum Science and Technology (Nos. 2021ZD0301800 and 2021ZD0301900), the New Cornerstone Science Foundation, and CAS Project for Young Scientists in Basic Research (Grant No. YSBR-057). We thank the HPC-ITP for the technical support and generous allocation of CPU time.

* These authors contributed equally to this work.

† w.li@itp.ac.cn

‡ g.su@ucas.ac.cn

- [1] H. Sun, M. Huo, X. Hu, J. Li, Z. Liu, Y. Han, L. Tang, Z. Mao, P. Yang, B. Wang, J. Cheng, D.-X. Yao, G.-M. Zhang, and M. Wang, Signatures of superconductivity near 80 K in a nickelate under high pressure, *Nature* **621**, 493 (2023).
- [2] Z. Liu, M. Huo, J. Li, Q. Li, Y. Liu, Y. Dai, X. Zhou, J. Hao, Y. Lu, M. Wang, and H.-H. Wen, Electronic correlations and energy gap in the bilayer nickelate $\text{La}_3\text{Ni}_2\text{O}_7$ (2023), [arXiv:2307.02950](https://arxiv.org/abs/2307.02950) [cond-mat.supr-con].
- [3] J. Hou, P. T. Yang, Z. Y. Liu, J. Y. Li, P. F. Shan, L. Ma, G. Wang, N. N. Wang, H. Z. Guo, J. P. Sun, Y. Uwatoko, M. Wang, G. M. Zhang, B. S. Wang, and J. G. Cheng, Emergence of high-temperature superconducting phase in the pressurized $\text{La}_3\text{Ni}_2\text{O}_7$ crystals (2023), [arXiv:2307.09865](https://arxiv.org/abs/2307.09865) [cond-mat.supr-con].
- [4] Y. Zhang, D. Su, Y. Huang, H. Sun, M. Huo, Z. Shan, K. Ye, Z. Yang, R. Li, M. Smidman, M. Wang, L. Jiao, and H. Yuan, High-temperature superconductivity with zero-resistance and strange metal behavior in $\text{La}_3\text{Ni}_2\text{O}_7$ (2023), [arXiv:2307.14819](https://arxiv.org/abs/2307.14819) [cond-mat.supr-con].
- [5] J. Yang, H. Sun, X. Hu, Y. Xie, T. Miao, H. Luo, H. Chen, B. Liang, W. Zhu, G. Qu, C.-Q. Chen, M. Huo, Y. Huang, S. Zhang, F. Zhang, F. Yang, Z. Wang, Q. Peng, H. Mao, G. Liu, Z. Xu, T. Qian, D.-X. Yao, M. Wang, L. Zhao, and X. J. Zhou, Orbital-dependent electron correlation in double-layer nickelate $\text{La}_3\text{Ni}_2\text{O}_7$ (2023), [arXiv:2309.01148](https://arxiv.org/abs/2309.01148) [cond-mat.supr-con].
- [6] M. Zhang, C. Pei, Q. Wang, Y. Zhao, C. Li, W. Cao, S. Zhu, J. Wu, and Y. Qi, Effects of pressure and doping on Ruddlesden-Popper phases $\text{La}_{n+1}\text{Ni}_n\text{O}_{3n+1}$ (2023), [arXiv:2309.01651](https://arxiv.org/abs/2309.01651) [cond-mat.supr-con].
- [7] G. Wang, N. Wang, J. Hou, L. Ma, L. Shi, Z. Ren, Y. Gu, X. Shen, H. Ma, P. Yang, Z. Liu, H. Guo, J. Sun, G. Zhang, J. Yan, B. Wang, Y. Uwatoko, and J. Cheng, Pressure-induced superconductivity in polycrystalline $\text{La}_3\text{Ni}_2\text{O}_7$ (2023), [arXiv:2309.17378](https://arxiv.org/abs/2309.17378) [cond-mat.supr-con].
- [8] G. Wang, N. Wang, Y. Wang, L. Shi, X. Shen, J. Hou, H. Ma, P. Yang, Z. Liu, H. Zhang, X. Dong, J. Sun, B. Wang, K. Jiang, J. Hu, Y. Uwatoko, and J. Cheng, Observation of high-temperature superconductivity in the high-pressure tetragonal phase of $\text{La}_2\text{PrNi}_2\text{O}_{7-\delta}$ (2023), [arXiv:2311.08212](https://arxiv.org/abs/2311.08212) [cond-mat.supr-con].
- [9] Z. Luo, X. Hu, M. Wang, W. Wú, and D.-X. Yao, Bilayer two-orbital model of $\text{La}_3\text{Ni}_2\text{O}_7$ under pressure, *Phys. Rev. Lett.* **131**, 126001 (2023).
- [10] Y. Zhang, L.-F. Lin, A. Moreo, and E. Dagotto, Electronic structure, orbital-selective behavior, and magnetic tendencies in the bilayer nickelate superconductor $\text{La}_3\text{Ni}_2\text{O}_7$ under pressure (2023), [arXiv:2306.03231](https://arxiv.org/abs/2306.03231) [cond-mat.supr-con].
- [11] Q.-G. Yang, D. Wang, and Q.-H. Wang, Possible s_{\pm} -wave superconductivity in $\text{La}_3\text{Ni}_2\text{O}_7$, *Phys. Rev. B* **108**, L140505 (2023).
- [12] F. Lechermann, J. Gondolf, S. Bötzel, and I. M. Eremin, Electronic correlations and superconducting instability in $\text{La}_3\text{Ni}_2\text{O}_7$ under high pressure (2023), [arXiv:2306.05121](https://arxiv.org/abs/2306.05121) [cond-mat.str-el].
- [13] H. Sakakibara, N. Kitamine, M. Ochi, and K. Kuroki, Possible high T_c superconductivity in $\text{La}_3\text{Ni}_2\text{O}_7$ under high pressure through manifestation of a nearly-half-filled bilayer Hubbard model (2023), [arXiv:2306.06039](https://arxiv.org/abs/2306.06039) [cond-mat.supr-con].
- [14] Y. Gu, C. Le, Z. Yang, X. Wu, and J. Hu, Effective model and pairing tendency in bilayer Ni-based superconductor $\text{La}_3\text{Ni}_2\text{O}_7$ (2023), [arXiv:2306.07275](https://arxiv.org/abs/2306.07275) [cond-mat.supr-con].
- [15] Y. Shen, M. Qin, and G.-M. Zhang, Effective bi-layer model Hamiltonian and density-matrix renormalization group study for the high- T_c superconductivity in $\text{La}_3\text{Ni}_2\text{O}_7$ under high pressure, *Chinese Physics Letters* **40**, 127401 (2023).
- [16] V. Christiansson, F. Petocchi, and P. Werner, Correlated electronic structure of $\text{La}_3\text{Ni}_2\text{O}_7$ under pressure, *Phys. Rev. Lett.* **131**, 206501 (2023).
- [17] D. A. Shilenko and I. V. Leonov, Correlated electronic structure, orbital-selective behavior, and magnetic correlations in double-layer $\text{La}_3\text{Ni}_2\text{O}_7$ under pressure, *Phys. Rev. B* **108**, 125105 (2023).
- [18] W. Wú, Z. Luo, D.-X. Yao, and M. Wang, Charge transfer and zhang-rice singlet bands in the nickelate superconductor $\text{La}_3\text{Ni}_2\text{O}_7$ under pressure (2023), [arXiv:2307.05662](https://arxiv.org/abs/2307.05662) [cond-mat.str-el].
- [19] Y. Cao and Y. feng Yang, Flat bands promoted by hund's rule coupling in the candidate double-layer high-temperature superconductor $\text{La}_3\text{Ni}_2\text{O}_7$ (2023), [arXiv:2307.06806](https://arxiv.org/abs/2307.06806) [cond-mat.supr-con].
- [20] X. Chen, P. Jiang, J. Li, Z. Zhong, and Y. Lu, Critical charge and spin instabilities in superconducting $\text{La}_3\text{Ni}_2\text{O}_7$ (2023), [arXiv:2307.07154](https://arxiv.org/abs/2307.07154) [cond-mat.supr-con].
- [21] Y.-B. Liu, J.-W. Mei, F. Ye, W.-Q. Chen, and F. Yang, The s_{\pm} -wave pairing and the destructive role of apical-oxygen deficiencies in $\text{La}_3\text{Ni}_2\text{O}_7$ under pressure (2023), [arXiv:2307.10144](https://arxiv.org/abs/2307.10144) [cond-mat.supr-con].
- [22] C. Lu, Z. Pan, F. Yang, and C. Wu, Interlayer coupling driven high-temperature superconductivity in $\text{La}_3\text{Ni}_2\text{O}_7$ under pressure (2023), [arXiv:2307.14965](https://arxiv.org/abs/2307.14965) [cond-mat.supr-con].
- [23] Y. Zhang, L.-F. Lin, A. Moreo, T. A. Maier, and E. Dagotto, Structural phase transition, s_{\pm} -wave pairing and magnetic stripe order in the bilayered nickelate superconductor $\text{La}_3\text{Ni}_2\text{O}_7$ under pressure (2023), [arXiv:2307.15276](https://arxiv.org/abs/2307.15276) [cond-mat.supr-con].
- [24] H. Oh and Y.-H. Zhang, Type II t - J model and shared antiferromagnetic spin coupling from Hund's rule in superconducting $\text{La}_3\text{Ni}_2\text{O}_7$ (2023), [arXiv:2307.15706](https://arxiv.org/abs/2307.15706) [cond-mat.str-el].
- [25] Z. Liao, L. Chen, G. Duan, Y. Wang, C. Liu, R. Yu, and Q. Si, Electron correlations and superconductivity in $\text{La}_3\text{Ni}_2\text{O}_7$ under pressure tuning (2023), [arXiv:2307.16697](https://arxiv.org/abs/2307.16697) [cond-mat.supr-con].
- [26] X.-Z. Qu, D.-W. Qu, J. Chen, C. Wu, F. Yang, W. Li, and G. Su,

- Bilayer t - J - J_{\perp} model and magnetically mediated pairing in the pressurized nickelate $\text{La}_3\text{Ni}_2\text{O}_7$ (2023), [arXiv:2307.16873 \[cond-mat.str-el\]](#).
- [27] Y.-f. Yang, G.-M. Zhang, and F.-C. Zhang, Interlayer valence bonds and two-component theory for high- T_c superconductivity of $\text{La}_3\text{Ni}_2\text{O}_7$ under pressure, *Phys. Rev. B* **108**, L201108 (2023).
- [28] K. Jiang, Z. Wang, and F.-C. Zhang, High temperature superconductivity in $\text{La}_3\text{Ni}_2\text{O}_7$ (2023), [arXiv:2308.06771 \[cond-mat.supr-con\]](#).
- [29] Y. Zhang, L.-F. Lin, A. Moreo, T. A. Maier, and E. Dagotto, Trends in electronic structures and s_{\pm} -wave pairing for the rare-earth series in bilayer nickelate superconductor $R_3\text{Ni}_2\text{O}_7$, *Phys. Rev. B* **108**, 165141 (2023).
- [30] J. Huang, Z. D. Wang, and T. Zhou, Impurity and vortex states in the bilayer high-temperature superconductor $\text{La}_3\text{Ni}_2\text{O}_7$, *Phys. Rev. B* **108**, 174501 (2023).
- [31] Q. Qin and Y.-f. Yang, High- T_c superconductivity by mobilizing local spin singlets and possible route to higher T_c in pressurized $\text{La}_3\text{Ni}_2\text{O}_7$, *Phys. Rev. B* **108**, L140504 (2023).
- [32] Y.-H. Tian, Y. Chen, J.-M. Wang, R.-Q. He, and Z.-Y. Lu, Correlation effects and concomitant two-orbital s_{\pm} -wave superconductivity in $\text{La}_3\text{Ni}_2\text{O}_7$ under high pressure (2023), [arXiv:2308.09698 \[cond-mat.supr-con\]](#).
- [33] D.-C. Lu, M. Li, Z.-Y. Zeng, W. Hou, J. Wang, F. Yang, and Y.-Z. You, Superconductivity from doping symmetric mass generation insulators: Application to $\text{La}_3\text{Ni}_2\text{O}_7$ under pressure (2023), [arXiv:2308.11195 \[cond-mat.str-el\]](#).
- [34] R. Jiang, J. Hou, Z. Fan, Z.-J. Lang, and W. Ku, Pressure driven screening of Ni spin results in cuprate-like high- T_c superconductivity in $\text{La}_3\text{Ni}_2\text{O}_7$ (2023), [arXiv:2308.11614 \[cond-mat.supr-con\]](#).
- [35] N. Kitamine, M. Ochi, and K. Kuroki, Theoretical designing of multiband nickelate and palladate superconductors with $d^{8+\delta}$ configuration (2023), [arXiv:2308.12750 \[cond-mat.supr-con\]](#).
- [36] Z. Luo, B. Lv, M. Wang, W. Wú, and D. xin Yao, High- T_C superconductivity in $\text{La}_3\text{Ni}_2\text{O}_7$ based on the bilayer two-orbital t - J model (2023), [arXiv:2308.16564 \[cond-mat.supr-con\]](#).
- [37] J.-X. Zhang, H.-K. Zhang, Y.-Z. You, and Z.-Y. Weng, Strong pairing originated from an emergent \mathbb{Z}_2 berry phase in $\text{La}_3\text{Ni}_2\text{O}_7$ (2023), [arXiv:2309.05726 \[cond-mat.str-el\]](#).
- [38] Z. Pan, C. Lu, F. Yang, and C. Wu, Effect of rare-earth element substitution in superconducting $R_3\text{Ni}_2\text{O}_7$ under pressure (2023), [arXiv:2309.06173 \[cond-mat.supr-con\]](#).
- [39] H. Sakakibara, M. Ochi, H. Nagata, Y. Ueki, H. Sakurai, R. Matsumoto, K. Terashima, K. Hirose, H. Ohta, M. Kato, Y. Takano, and K. Kuroki, Theoretical analysis on the possibility of superconductivity in a trilayer Ruddlesden-Popper nickelate $\text{La}_4\text{Ni}_3\text{O}_{10}$ under pressure and its experimental examination: comparison with $\text{La}_3\text{Ni}_2\text{O}_7$ (2023), [arXiv:2309.09462 \[cond-mat.supr-con\]](#).
- [40] H. Lange, L. Homeier, E. Demler, U. Schollwöck, A. Bohrdt, and F. Grusdt, Pairing dome from an emergent Feshbach resonance in a strongly repulsive bilayer model (2023), [arXiv:2309.13040 \[cond-mat.str-el\]](#).
- [41] B. Geisler, J. J. Hamlin, G. R. Stewart, R. G. Hennig, and P. J. Hirschfeld, Structural transitions, octahedral rotations, and electronic properties of $A_3\text{Ni}_2\text{O}_7$ rare-earth nickelates under high pressure (2023), [arXiv:2309.15078 \[cond-mat.supr-con\]](#).
- [42] H. Yang, H. Oh, and Y.-H. Zhang, Strong pairing from doping-induced Feshbach resonance and second Fermi liquid through doping a bilayer spin-one Mott insulator: application to $\text{La}_3\text{Ni}_2\text{O}_7$ (2023), [arXiv:2309.15095 \[cond-mat.str-el\]](#).
- [43] L. C. Rhodes and P. Wahl, Structural routes to stabilise superconducting $\text{La}_3\text{Ni}_2\text{O}_7$ at ambient pressure (2023), [arXiv:2309.15745 \[cond-mat.supr-con\]](#).
- [44] H. Lange, L. Homeier, E. Demler, U. Schollwöck, F. Grusdt, and A. Bohrdt, Feshbach resonance in a strongly repulsive bilayer model: a possible scenario for bilayer nickelate superconductors (2023), [arXiv:2309.15843 \[cond-mat.str-el\]](#).
- [45] H. LaBollita, V. Pardo, M. R. Norman, and A. S. Botana, Electronic structure and magnetic properties of $\text{La}_3\text{Ni}_2\text{O}_7$ under pressure (2023), [arXiv:2309.17279 \[cond-mat.str-el\]](#).
- [46] U. Kumar, C. Melnick, and G. Kotliar, Softening of dd excitation in the resonant inelastic x-ray scattering spectra as a signature of Hund's coupling in nickelates (2023), [arXiv:2310.00983 \[cond-mat.str-el\]](#).
- [47] T. Kaneko, H. Sakakibara, M. Ochi, and K. Kuroki, Pair correlations in the two-orbital Hubbard ladder: Implications on superconductivity in the bilayer nickelate (2023), [arXiv:2310.01952 \[cond-mat.supr-con\]](#).
- [48] C. Lu, Z. Pan, F. Yang, and C. Wu, Interplay of two E_g orbitals in superconducting $\text{La}_3\text{Ni}_2\text{O}_7$ under pressure (2023), [arXiv:2310.02915 \[cond-mat.supr-con\]](#).
- [49] S. Rye, N. Witt, and T. O. Wehling, Critical role of interlayer dimer correlations in the superconductivity of $\text{La}_3\text{Ni}_2\text{O}_7$ (2023), [arXiv:2310.17465 \[cond-mat.supr-con\]](#).
- [50] H. Schlömer, U. Schollwöck, F. Grusdt, and A. Bohrdt, Superconductivity in the pressurized nickelate $\text{La}_3\text{Ni}_2\text{O}_7$ in the vicinity of a BEC-BCS crossover (2023), [arXiv:2311.03349 \[cond-mat.str-el\]](#).
- [51] J. Chen, F. Yang, and W. Li, Orbital-selective superconductivity in the pressurized bilayer nickelate $\text{La}_3\text{Ni}_2\text{O}_7$: An infinite projected entangled-pair state study (2023), [arXiv:2311.05491 \[cond-mat.str-el\]](#).
- [52] H. Liu, C. Xia, S. Zhou, and H. Chen, Role of crystal-field-splitting and long-range-hoppings on superconducting pairing symmetry of $\text{La}_3\text{Ni}_2\text{O}_7$ (2023), [arXiv:2311.07316 \[cond-mat.supr-con\]](#).
- [53] Z. Ouyang, J.-M. Wang, J.-X. Wang, R.-Q. He, L. Huang, and Z.-Y. Lu, Hund electronic correlation in $\text{La}_3\text{Ni}_2\text{O}_7$ under high pressure (2023), [arXiv:2311.10066 \[cond-mat.str-el\]](#).
- [54] W.-X. Chang, S. Guo, Y.-Z. You, and Z.-X. Li, Fermi surface symmetric mass generation: a quantum monte-carlo study (2023), [arXiv:2311.09970 \[cond-mat.str-el\]](#).
- [55] S. Hirthe, T. Chalopin, D. Bourgund, P. Bojović, A. Bohrdt, E. Demler, F. Grusdt, I. Bloch, and T. A. Hilker, Magnetically mediated hole pairing in fermionic ladders of ultracold atoms, *Nature* **613**, 463 (2023).
- [56] W. Li, S.-J. Ran, S.-S. Gong, Y. Zhao, B. Xi, F. Ye, and G. Su, Linearized tensor renormalization group algorithm for the calculation of thermodynamic properties of quantum lattice models, *Phys. Rev. Lett.* **106**, 127202 (2011).
- [57] B.-B. Chen, L. Chen, Z. Chen, W. Li, and A. Weichselbaum, Exponential thermal tensor network approach for quantum lattice models, *Phys. Rev. X* **8**, 031082 (2018).
- [58] Q. Li, Y. Gao, Y.-Y. He, Y. Qi, B.-B. Chen, and W. Li, Tangent space approach for thermal tensor network simulations of the 2D Hubbard model, *Phys. Rev. Lett.* **130**, 226502 (2023).
- [59] A. Georges, L. d. Medici, and J. Mravlje, Strong Correlations from Hund's Coupling, *Annual Review of Condensed Matter Physics* **4**, 137 (2013).
- [60] S. R. White, Density matrix formulation for quantum renormalization groups, *Phys. Rev. Lett.* **69**, 2863 (1992).
- [61] U. Schollwöck, The Density-Matrix Renormalization Group in the Age of Matrix Product States, *Ann. Phys.* **326**, 96 (2011).
- [62] A. Weichselbaum, Non-Abelian Symmetries in Tensor Networks : A Quantum Symmetry Space Approach, *Ann. Phys.*

- 327, 2972 (2012).
- [63] A. Weichselbaum, X-symbols for non-Abelian symmetries in tensor networks, *Phys. Rev. Research* **2**, 023385 (2020).
 - [64] M. Fishman, S. R. White, and E. M. Stoudenmire, The ITensor Software Library for Tensor Network Calculations, *SciPost Phys. Codebases* , 4 (2022).
 - [65] M. Fishman, S. R. White, and E. M. Stoudenmire, Codebase release 0.3 for ITensor, *SciPost Phys. Codebases* , 4 (2022).
 - [66] In Supplementary Sec. I, we provide the process for extrapolating the SC order parameter Δ_z as a function of J_\perp and t_\perp to the infinite- D limit. In Sec. II, we present the same process to obtain the extrapolated results for the substitution of rare-earth elements in nickelate $R_3Ni_2O_7$.
 - [67] A. Gleis, J.-W. Li, and J. von Delft, Controlled bond expansion for density matrix renormalization group ground state search at single-site costs, *Phys. Rev. Lett.* **130**, 246402 (2023).
 - [68] A. Wietek, Fragmented cooper pair condensation in striped superconductors, *Phys. Rev. Lett.* **129**, 177001 (2022).

Supplementary Materials for

**Roles of Hund's Rule and Hybridization in the Two-orbital Model
for High- T_c Superconductivity in the Bilayer Nickelate**

Qu *et al.*

I. DMRG DETAILS AND CONVERGENCE CHECK

Since the largest coupling coefficient is the ferromagnetic J_H , which competes with the AF background and hybridization in most instances we considered, the two-orbital model might stuck in local minimum during DMRG sweeps. There are several tricks to avoid this predicament and get the real ground state.

The first way is to employ less symmetry. Although the model respects $U(1)_{\text{charge}} \times SU(2)_{\text{spin}}$ symmetry, one may choose to use $U(1)_{\text{charge}} \times U(1)_{\text{spin}}$ instead and permit finite magnetization for the first few DMRG sweeps. The reason is that $U(1)_{\text{charge}} \times U(1)_{\text{spin}}$ DMRG sustains larger local variation space and leads to more robust performance. Anyway, $\langle S_i^z \rangle \sim 10^{-7}$ is ensured for the final converged results.

The second method is to perform three-site or even four-site DMRG. If $U(1)_{\text{charge}} \times SU(2)_{\text{spin}}$ symmetry is exploited, we composite the two orbitals on the same site and deal with $d = 9$ local Hilbert spaces, which is equivalently a four-site update scheme. CBE-DMRG [67] is employed to significantly reduce the computational cost.

The third skill is to adopt the ground state MPS which is obtained from a closely related Hamiltonian as the initialized state. For example, taken the ground state MPS of $J_H = 1.1$ eV, we truncate it to $D = 1,000$ $U(1)_{\text{charge}} \times U(1)_{\text{spin}}$ states and use it as the initialized state for the calculation of $J_H = 1.3$ eV system.

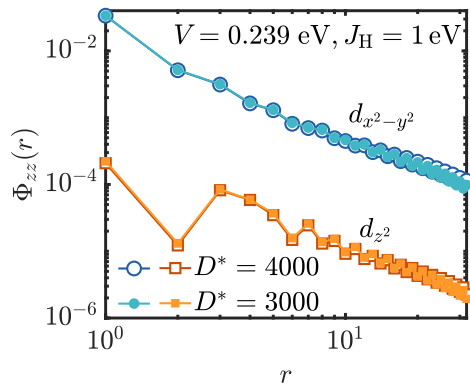


FIG. S1. Interlayer pair correlation Φ_{zz} with different kept multiplets.

We check the convergence of DMRG calculations in Fig S1. Keeping realistic parameters, interlayer pair correlation obtained from $D^* = 3,000$ and $4,000$ $U(1)_{\text{charge}} \times SU(2)_{\text{spin}}$ multiplets show excellent consistence up to distance $r = 20$.

II. ADDITIONAL DMRG RESULTS FOR ORBITAL-SELECTIVE SUPERCONDUCTIVITY

We show in this section more DMRG results to support the conclusion in the main text.

In Fig. S2(a) we confirm the exponentially decay behavior of spin correlation and single-particle Green's function, ensuring a typical Luther-Emery liquid behavior.

To describe the hole bunching in the two-orbital ladder, we also calculate $g_h^{(2)} = \langle h_{i,\mu=1} h_{j,\mu=-1} \rangle_\beta / (\langle h_{i,\mu=1} \rangle_\beta \langle h_{j,\mu=-1} \rangle_\beta) - 1$ with $h_{i,\mu}$ the hole number operator for $d_{x^2-y^2}$ or d_{z^2} orbital. More precisely, we call it type I structure if site i, j are in the same unit cell while type II if site i, j are in the nearest neighbor unit cell, as illustrated in the inset of Fig. S2(b). Positive $g_h^{(2)}$ indicates attractive hole correlation between the specified two sites and vice versa. It is clear in Fig. S2(b) that holes in $d_{x^2-y^2}$ orbital tend to bunch in the same unit cell while repel each other if they are in different unit cell. However, holes in d_{z^2} orbital always repel each other and thus can hardly pair up. Serving as a corroboration, superconductivity of d_{z^2} orbital is thus possibly to be subordinate while the $d_{x^2-y^2}$ orbital is responsible for the robust dominant SC order in $\text{La}_3\text{Ni}_2\text{O}_7$.

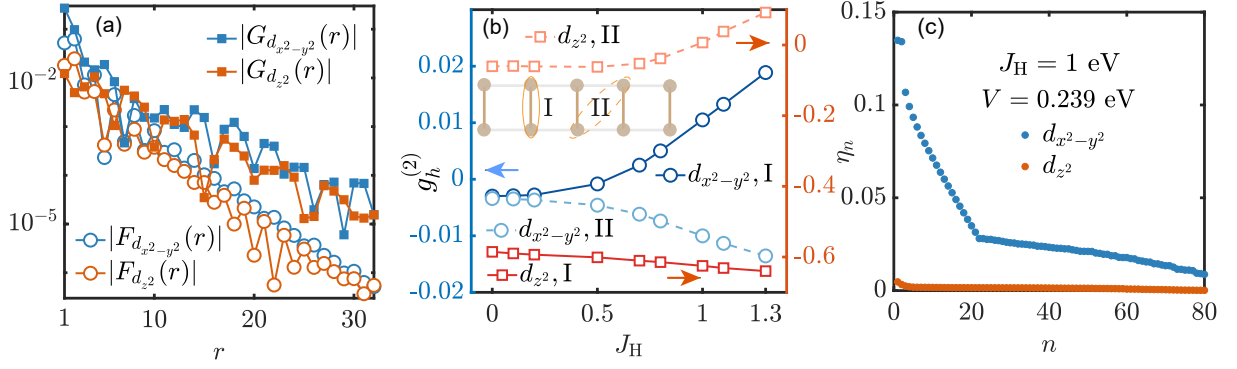


FIG. S2. (a) Spin correlation and single-particle Green's function at $V = 0.239$ eV, $J_H = 1$ eV. (b) Interlayer statistical hole correlation $g_h^{(2)}$ (see definition below) for both orbitals. (c) First $n = 80$ eigenvalues of pair correlation density matrix.

To further systematically study the orbital difference between two orbitals, we adopt a newly proposed method [68] to analyze the condensation of Cooper pairs in the two-orbital model. Density matrix of singlet pairing is defined as $\rho_S(\mathbf{r}_i, \alpha | \mathbf{r}_j, \beta) = \langle \hat{\Delta}_\alpha^\dagger(\mathbf{r}_i) \hat{\Delta}_\beta(\mathbf{r}_j) \rangle$, where $\alpha, \beta = \{x, z\}$ denote the lattice bond and all-to-all pair correlation are taken into account. Eigen-spectrum of ρ_S characterizes the superconducting condensate fraction. Isolated eigenvalues above the continuous spectrum are considered as evidence for the condensation of Cooper pairs, indicating an off-diagonal long-range-order in the 2D limit. Fig. S2(c) manifests the eigen-spectrum η_n for the two orbitals with the first $n = 80$ eigenvalues. The spectrum of $d_{x^2-y^2}$ orbital demonstrates condensation clearly with two macroscopic occupied states (corresponding to two dominant isolated eigen-values.) On the contrary, eigen-spectrum of d_{z^2} orbital is featureless, suggesting an absence of superconductivity.

III. SUPERCONDUCTIVITY UPON FINE TUNING THE SITE ENERGY

In order to further verify the role of d_{z^2} orbital, we increase the difference of site energy between two orbitals to transfer more electrons to d_{z^2} orbital while keeping other realistic parameters of $\text{La}_3\text{Ni}_2\text{O}_7$, namely $n_e = 3/8$, $J_H = 1$ eV and $V = 0.239$ eV. In Fig. S3(a) we show that pair correlation of both orbitals are significantly enhanced while increasing $\Delta\varepsilon$. The resulted electron density, $\langle n_c \rangle$ for $d_{x^2-y^2}$ orbital and $\langle n_d \rangle$ for d_{z^2} orbital are shown in Fig. S3(b). AF interaction can be mediated to $d_{x^2-y^2}$ orbital more efficiently as d_{z^2} orbital approaching half-filling, evidenced by F_\perp^c in Fig. S3(c). On the contrary, the intralayer spin correlation F_\parallel^c gets suppressed. The enhancement of $d_{x^2-y^2}$ orbital originates from the increasing of interlayer AF correlation, which is mediated more effectively via localized d_{z^2} moments by the Hund's rule coupling. However, based on the analysis in the main text, we attribute the superconductivity of d_{z^2} orbital to the proximity effect.

It thus makes sense to further reduce the two orbital model to a single orbital effective model. Notice that Hund's rule coupling J_H is crucial for the emergence of SC and d_{z^2} orbital is nearly half-filled and only contributes to SC indirectly, one may safely "freeze" d_{z^2} orbital as a local moment and act as a mediation to pass interlayer exchange for $d_{x^2-y^2}$ orbital through J_H . That

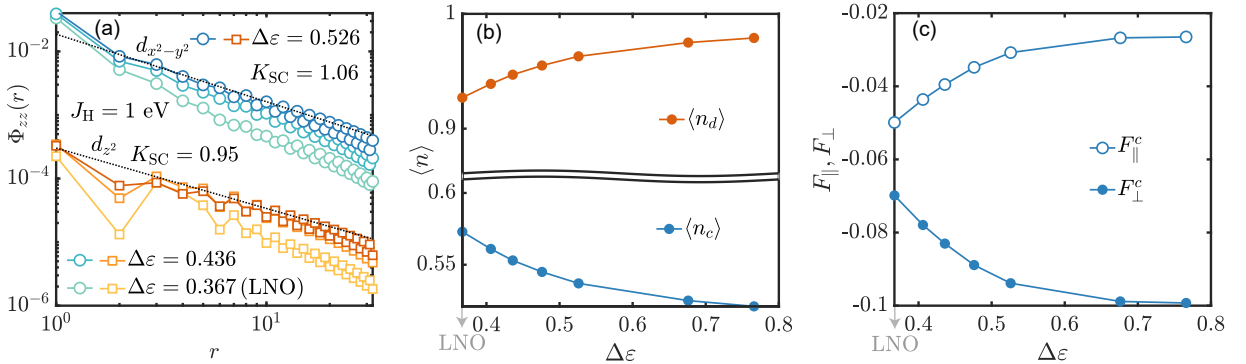


FIG. S3. (a) Interlayer pair correlation for $d_{x^2-y^2}$ and d_{z^2} orbitals while adjusting offset of site energy $\Delta\varepsilon \equiv \varepsilon_c - \varepsilon_d$. $\Delta\varepsilon = 0.367$ eV corresponds to the realistic parameter for $\text{La}_3\text{Ni}_2\text{O}_7$ (LNO). (b) Electron densities of the two e_g orbitals while adjusting $\Delta\varepsilon$. (c) Interlayer and intralayer spin correlation (F_\perp^c and F_\parallel^c). Realistic parameter is on the leftmost for both (b) and (c).

way, under large J_H the two orbital model would reduce to a t - J - J_\perp model, which reads,

$$H = -t \sum_{\langle i,j \rangle, \mu, \sigma} (c_{i,\mu,\sigma}^\dagger c_{j,\mu,\sigma} + H.c.) + J \sum_{\langle i,j \rangle, \mu} (\mathbf{S}_{i,\mu}^c \cdot \mathbf{S}_{j,\mu}^c - \frac{1}{4} n_{i,\mu} n_{j,\mu}) + J_\perp \sum_i \mathbf{S}_{i,\mu=1}^c \cdot \mathbf{S}_{i,\mu=-1}^c, \quad (\text{S1})$$

where all the operators act on $d_{x^2-y^2}$ orbital. Such minimal effective model is studied in a previous work [26].